

# Pre-equilibrium mechanisms in the $^{93}\text{Nb}(\vec{p},\alpha)$ inclusive reaction at incident energies from 65 to 160 MeV

S. S. Dimitrova,<sup>1,2,\*</sup> A. A. Cowley,<sup>3,4,†</sup> E. V. Zemlyanaya,<sup>2</sup> and K. V. Lukyanov<sup>2</sup>

<sup>1</sup>*Institute for Nuclear Research and Nuclear Energy,  
Bulgarian Academy of Sciences, 1784 Sofia, Bulgaria*

<sup>2</sup>*Joint Institute for Nuclear Research, 141980 Dubna, Russia*

<sup>3</sup>*Department of Physics, Stellenbosch University, Private Bag X1, Matieland, 7602, South Africa*

<sup>4</sup>*Themba Laboratory for Accelerator Based Sciences,  
P O Box 722, Somerset West 7129, South Africa*

The reaction mechanism of pre-equilibrium proton-induced  $\alpha$ -particle emission from  $^{93}\text{Nb}$  at an incident energy of 100 MeV was investigated with polarized projectiles. A formalism based on the statistical multistep direct emission model of Feshbach, Kerman and Koonin was found to give a reasonably good reproduction of cross section and analyzing power angular distributions at various emission energies. Existing experimental distributions for the same reaction at an incident energy of 65 MeV were also analyzed with the same model. The incident-energy variation from 65 MeV up to 160 MeV was found to be consistent with the predictions of the basic model. However, whereas knockout of an  $\alpha$  cluster is the dominant reaction mechanism in the final stage at the lowest- and highest incident energies, at 100 MeV a pickup process competes with comparable intensity in yield.

PACS numbers: PACS number(s): 25.40.Hs, 24.50.+g, 24.60.Gv, 24.70.+s

## I. INTRODUCTION

Angular- and energy distributions of nucleons emitted in proton-induced pre-equilibrium reactions [1] in the incident energy range up to 200 MeV are described well in terms of several related quantum-mechanical formulations [1, 2]. Of the available models, the statistical multistep direct emission (SMDE) theory of Feshbach, Kerman and Koonin (FKK) [3] has been extensively and successfully compared with experimental results over a large target mass and incident energy range [1, 4–7].

Although the emission of composite particles in pre-equilibrium reactions, such as  $^3\text{He}$  and  $\alpha$  particles, could be a more complicated process than the emission of nucleons, it is nevertheless reasonable to expect that the relevant reaction mechanism should be an intrinsic part of the basic process described, for example, by the FKK theory.

In earlier work on proton-induced emission of  $^3\text{He}$  into the continuum, we attempted to identify the simplest dominant reaction process in the incident energy range below 200 MeV [8–11]. Because analyzing power angular distributions are more sensitive to details of the reaction mechanism than those of the cross section, polarized projectiles proved to be especially valuable for these studies. It was found that the incident-energy evolution of the characteristics of the analyzing power angular distributions is consistent [9–11] with a simple two-nucleon pickup process convoluted with the SMDE mechanism. Unfortunately, the usefulness of the analyzing power to unravel details of the reaction mechanism diminishes towards the upper end of the energy range. The reason is

that the analyzing power tends to have lower values at higher incident energies, essentially disappearing at 200 MeV [12] even at forward angles. The observed quenching of the analyzing power as a function of increasing incident energy is understood [13] as an inherent feature of direct pickup.

The present study provides further insight into the reaction mechanism of emission of  $\alpha$  particles. Of course, three-nucleon pickup as well as knockout could both be important processes in proton-induced emission of  $\alpha$  particles. However, in one of our early investigations with unpolarized projectiles [14] at incident energies between 120 and 200 MeV the experimental cross section angular distributions of the reaction  $^{59}\text{Co}(p,\alpha)$  at various emission energies were fairly reliably reproduced by invoking only a knockout mechanism in the theoretical analysis. Also, in our recent paper [15] on the reaction  $^{93}\text{Nb}(\vec{p},\alpha)$  at an incident energy of 160 MeV, we found that best agreement of the theoretical predictions with experimental cross section and analyzing power angular distributions is obtained if knockout is assumed as the dominant mechanism. While keeping in mind these earlier results, in the present study we again consider the possible participation of both mechanisms – pickup as well as knockout – in the pre-equilibrium  $(p,\alpha)$  reaction at the lower incident energies explored now.

The motivation for the present work is to investigate the incident-energy dependence of the  $^{93}\text{Nb}(\vec{p},\alpha)$  reaction to lower values (down to 65 MeV) than explored in our previous investigation at 160 MeV. For this purpose we use new experimental data at 100 MeV together with existing published angular distributions at an incident energy of 65 MeV [16]. We assume implicitly that the reaction mechanism for the target nucleus  $^{93}\text{Nb}$  is representative of nuclei in general. Clearly, trivial differences, which relate to structure details of a particular nuclear

\* sevdim@inrne.bas.bg

† aac@sun.ac.za

species, should be observable.

We now find, as in our earlier work and as would be expected, that the extended FKK theory gives a very good reproduction of the cross section and analyzing power angular distributions for the  $^{93}\text{Nb}(\vec{p},\alpha)$  reaction at 100 MeV as well as at 65 MeV incident energy. However, an unexpected and interesting feature of the new investigation is that, at an incident energy of 100 MeV, a pickup mechanism now competes strongly with a knockout process. Evidently, this is in strong contrast with the trend at both higher (160 MeV [15]) and lower (65 MeV; also from this work) incident energies where knockout appears to be overwhelmingly dominant.

This paper has the following structure: In Sec. II the experimental technique at an incident energy of 100 MeV is described. This is followed with a summary of the theoretical ideas in Sec. III. In Sec. IV the results are shown and discussed. Finally, in Sec. V a summary and conclusions are presented.

In this paper we often use, for example, the notation  $(p,\alpha)$  instead of  $(\vec{p},\alpha)$  which is appropriate. As we refer mostly to reactions induced by polarized projectiles, the meaning should be clear from the context.

## II. EXPERIMENTAL PROCEDURE

The reaction  $^{93}\text{Nb}(\vec{p},\alpha)$  at an incident energy of  $100 \pm 0.5$  MeV was measured at iThemba LABS (at the time known as the National Accelerator Centre) in Faure, South Africa. A description of the facility is available in Ref. [17].

Cross sections and analyzing distributions were measured in the same experiment [9] as those for  $^{93}\text{Nb}(\vec{p},^3\text{He})$ , but the present data were extracted at a much later date from the event-by-event records stored online. Only a brief summary of the fairly standard experimental technique is provided here for ease of reference.

Two detector telescopes, each consisting of a 500- $\mu\text{m}$  silicon surface-barrier detector followed by a NaI(Tl) crystal coupled to a phototube, were positioned at symmetric angles on opposite sides of the incident beam in a 1.5-m diameter scattering chamber. The telescopes were collimated to a solid angle acceptance of about 1.1 msr. The scattering-angle positions were set to an accuracy of better than  $0.2^\circ$  with respect to the incident beam.

Two self-supporting targets of naturally occurring niobium (100% in the isotope  $^{93}\text{Nb}$ ) of thicknesses of approximately 1 and 5  $\text{mg}/\text{cm}^2$  were used. The main systematic uncertainty in the cross section data – about 8% – originates from the absolute value of the target thickness and its uniformity.

The incident proton beam was polarized to a nominal value of 80% perpendicular to the reaction plane, and the direction of the polarization was switched at 5-s intervals during measurements. Variation between the degree of polarization for the two directions was less than 10%.

These values were monitored regularly by means of elastic scattering of the proton beam from a carbon target at a scattering angle where the analyzing power is large and known accurately.

The use of detector telescopes positioned symmetrically with respect to the incident proton beam, together with the switching of the polarization direction allows us to minimize systematic errors in the analyzing power measurements. The vector analyzing power is calculated from the expression [16], which follows from the standard Basel-Madison conventions, as

$$A_y = \frac{L - R}{P(L + R)}, \quad (1)$$

with

$$L = \sqrt{L_u R_d}, \quad (2)$$

and

$$R = \sqrt{L_d R_u}. \quad (3)$$

The average polarization of the beam is  $P$ . The summed counts in each detector for a given energy interval in the spectra are indicated by  $L$  (left) or  $R$  (right), with subscripts which indicate the spin direction of the projectile as either up ( $u$ ) or down ( $d$ ). The convention is as defined by a spectator facing along the momentum direction of the incident beam upstream from the target. Comparison of this formulation of analyzing power with the expression containing the specific values of the two orientations of the polarization [18] indicates that a 10% difference affects the measured value by only 1%.

Energy calibrations of the Si detectors were based on measurements from a  $^{228}\text{Th}$  source, and those of the NaI crystals were determined from proton scattering from a  $(\text{CH})_n$  target, adjusted for the difference in response of  $\alpha$  particles. The overall accuracy of the emission-energy scale is better than 4%. Cross sections and analyzing powers were binned in 4 MeV wide energy intervals.

## III. THEORETICAL ANALYSIS

We consider the  $(p,\alpha)$  inclusive reactions at incident energy of 100 MeV and 65 MeV as pre-equilibrium reactions. As in our previous studies on  $(p,^3\text{He})$  processes [8–11], we assume that this type of reaction occurs in a series of intranuclear  $N$ - $N$  steps preceding a final process in which the  $\alpha$  particle is emitted. The single step direct reaction can be a knockout of an  $\alpha$  cluster or a pickup of a triton. We will consider the contribution of both reaction mechanisms to the total double-differential cross section and analyzing power for different energies of the  $\alpha$  particle in the outgoing channel.

The theory applied to the  $(p,\alpha)$  reaction is based on the multistep direct theory of Feshbach, Kerman and Koonin (FKK) [3]. The extension of the FKK theory

from nucleon- to composite-particle emission has been presented often, and a recent description can be found in our previous paper [15].

The details of the methodology of the  $(p, \alpha)$  calculations are also described in Ref. [15], thus now we will just briefly outline the main expressions. We will emphasize specific subtleties needed for the adequate description of the reactions considered.

### A. Differential cross sections

The expression for the pre-equilibrium  $(p, \alpha)$  cross section is written as a sum of various steps as

$$\begin{aligned} \left( \frac{d^2\sigma}{d\Omega dE} \right)_{p,\alpha}^{\text{total}} &= \left( \frac{d^2\sigma}{d\Omega dE} \right)_{p,\alpha}^{1\text{-step}} \\ &+ \sum_{n=2}^{n_{\max}} \sum_{m=n-1}^{n+1} \int \frac{d\mathbf{k}_1}{(2\pi)^3} \int \frac{d\mathbf{k}_2}{(2\pi)^3} \cdots \int \frac{d\mathbf{k}_n}{(2\pi)^3} \\ &\times \left( \frac{d^2\sigma(\mathbf{k}_f, \mathbf{k}_n)}{d\Omega_f dE_f} \right) \times \left( \frac{d^2\sigma(\mathbf{k}_n, \mathbf{k}_{n-1})}{d\Omega_n dE_n} \right) \times \cdots \\ &\times \left( \frac{d^2\sigma(\mathbf{k}_2, \mathbf{k}_1)}{d\Omega_2 dE_2} \right) \times \left( \frac{d^2\sigma(\mathbf{k}_1, \mathbf{k}_i)}{d\Omega_1 dE_1} \right)_{p,N}, \end{aligned} \quad (4)$$

where  $\mathbf{k}_i$ ,  $\mathbf{k}_n$  and  $\mathbf{k}_f$  are the momenta of the initial,  $n^{\text{th}}$  and final steps. The number of reaction steps is indicated with the symbol  $n$ , the maximum number of reaction steps is  $n_{\max}$  and  $m$  is the exit mode. Therefore, in the present application, the cross section associated with  $m$  corresponds to the emission of an  $\alpha$  particle. All steps prior to the final emission are nucleon-nucleon collisions which originate from the initial projectile- $N$  cross section  $\left( \frac{d^2\sigma}{d\Omega_1 dE_1} \right)_{p,N}$ . Of course, the first term, which does not involve preceding nucleon collisions, is given in terms of the distorted-wave Born approximation (DWBA) by

$$\left( \frac{d^2\sigma}{d\Omega dE} \right)_{p,\alpha}^{1\text{-step}} = \sum_{N,L,J} \frac{(2J+1)}{\Delta E} \frac{d\sigma^{\text{DW}}}{d\Omega}(\theta, N, L, J, E), \quad (5)$$

at scattering angle  $\theta$ , where the summation runs over the target states with single-particle energies within a small interval  $(E - \Delta E/2, E + \Delta E/2)$  around the excitation energy  $E$  (in these particular calculations we adopted  $\Delta E = 4$  MeV to match the experimental energy bin). If the DWBA calculation is treated as a knockout, quantum numbers  $N, L$  and  $J$  refer to the  $\alpha$  cluster bound in the target, otherwise to those of the three-nucleon system which is picked up. The differential cross sections  $d\sigma^{\text{DW}}/d\Omega$  to particular  $(N, L, J)$  states are calculated using the code DWUCK4 [19].

A related formulation in terms of the DWBA holds for the initial projectile- $N$  interaction represented by  $\left( \frac{d^2\sigma}{d\Omega_1 dE_1} \right)_{p,N}$ . This is provided in, for example, Ref. [7].

The theoretical  $(p, p')$  and  $(p, p', p'')$  double-differential cross section distributions which are required to calculate the contributions of the second- and third-step processes were derived from Refs. [5, 14]. These cross section distributions were extracted by means of a FKK multistep direct reaction theory, which reproduces experimental inclusive  $(p, p')$  quantities [5] on target nuclei which are close to those needed for this work, and in an appropriate incident energy range. Interpolations and extrapolations in incident energy and target mass were introduced to match the specific requirements accurately.

Clearly, the formalism separates calculation of multi-step processes, such as one-step  $(p, \alpha)$ , two-step  $(p, p', \alpha)$ , and three-step  $(p, p', p'', \alpha)$  reactions. This can be expressed as

$$\frac{d^2\sigma}{d\Omega dE} = \left( \frac{d^2\sigma}{d\Omega dE} \right)^{1\text{-step}} + \left( \frac{d^2\sigma}{d\Omega dE} \right)^{2\text{-step}} + \cdots, \quad (6)$$

in which the relationship of the notation is linked clearly to the formulation given thus far.

In previous work [9, 10], intermediate steps which involve neutrons, such as  $(p, n, \alpha)$ , were not explicitly taken into account because we assumed that different nucleons may be treated on an equal footing in the multi-step part of the reaction. This meant that a simple renormalization of the  $(p, p')$  and  $(p, p', p'')$  cross sections should be introduced to correct for the influence of the intermediate counterparts which involve neutrons. In these present calculations we take into account explicitly the  $(p, n, \alpha)$  process by assuming that  $d^2\sigma^{(p,n)}/d\Omega dE = d^2\sigma^{(p,p')}/d\Omega dE$  and also the four possible combinations of two-step intranuclear collisions  $(p, x, x)$ ,  $x = n, p$  with  $d^2\sigma^{(p,x,x)}/d\Omega dE = d^2\sigma^{(p,p',p'')}/d\Omega dE$ .

### B. Analyzing power distributions

The extension of the FKK theory from cross sections to analyzing power is described by Bonetti *et al.* [20]. The multistep expression for the analyzing power becomes

$$A_{\text{multistep}} = \frac{A_1 \left( \frac{d^2\sigma}{d\Omega dE} \right)^{1\text{-step}} + A_2 \left( \frac{d^2\sigma}{d\Omega dE} \right)^{2\text{-step}} + \cdots}{\left( \frac{d^2\sigma}{d\Omega dE} \right)^{1\text{-step}} + \left( \frac{d^2\sigma}{d\Omega dE} \right)^{2\text{-step}} + \cdots}, \quad (7)$$

with  $A_i$ ,  $\{i = 1, 2, \dots\}$  referring to analyzing powers for the successive multisteps.

### C. Multi-step contributions to the cross section and analyzing power

In Fig. 1 the one-, two- and three-step contributions to the double-differential cross section and analyzing power as a function of scattering angle  $\theta$  for the  $^{93}\text{Nb}(p, \alpha)$  reaction at an incident energy of 100 MeV and an  $\alpha$ -particle

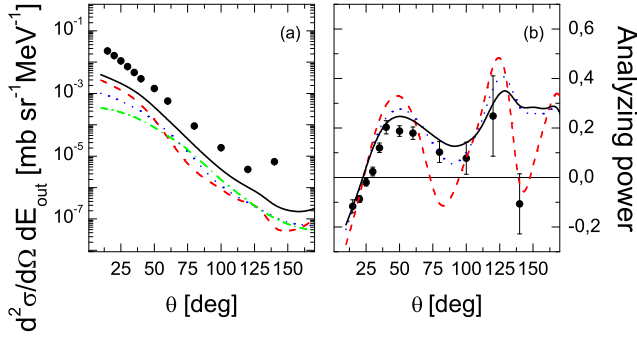


FIG. 1. (Color online) Double-differential cross section (a) and analyzing power (b) as a function of scattering angle  $\theta$  for the  $^{93}\text{Nb}(p,\alpha)$  reaction at an incident energy of 100 MeV and an  $\alpha$ -particle emission energy of 86 MeV. Results for only the pickup component of the reaction mechanism are used to display contributions of various steps. Theoretical cross section calculations for one step (---), two steps (.....) and three steps (- · - · -) are shown, with the sums of the contributions plotted as continuous curves. The experimental analyzing power distribution is compared with theoretical calculations for a one-step reaction (---), a one-step plus a two-step reaction (.....), and a one- plus two- plus three-step reaction (solid lines).

emission energy of 86 MeV are displayed. For the purpose of this illustration of the effect of contributions from various steps of the interaction, only the pickup component of the reaction mechanism is used.

For this particular case of energy transfer all three steps of the process contribute significantly to the double-differential cross section and lead to a reduction of the oscillatory behavior of the analyzing power associated with the first step. This effect can be understood qualitatively in terms of the formulation of the combined analyzing power of the contributing multisteps.

The theory predicts that the relative contribution of the first-step reaction decreases as the emission energy drops, with higher steps becoming progressively more important towards lower emission energy. This is a general feature of multistep calculations, as was also found in our previous work [8–11, 15]. Although the actual step which is dominant at a specific emission energy only influences the shape of the cross section relatively slightly, an appreciable contribution of higher steps affects the analyzing power distribution profoundly. The trend is that the analyzing power tends towards zero at lower emission energy where higher steps become more important.

#### D. Optical potentials in the DWBA calculation

As in our previous papers [11, 15], in the DWBA calculations we employ the microscopic optical potential which takes into account the interaction between the projectile and target, and between the ejectile and the heavy residual nucleus, respectively. The theoretical approach of the

microscopic optical potential is presented in Refs. [21–24] and successfully applied e.g. in Refs. [25–28] for the analysis of elastic scattering data of light exotic nuclei. We already described details about the optical potential calculations in Refs. [11, 15]. Here we give, briefly, the main equations.

In general, the potentials contain volume  $V$  and spin-orbit  $V_{\text{SO}}$  parts, which are both complex and expressed as

$$U(\mathbf{r}) = V(\mathbf{r}) + V_{\text{SO}}(\mathbf{r}) \mathbf{L} \cdot \mathbf{S}, \quad (8)$$

where  $\mathbf{r}$  the radius-vector connecting centers of the interacting nuclei,  $\mathbf{L}$  the angular momentum, and  $\mathbf{S}$  the intrinsic spin of the projectile. In the  $^4\text{He}$  case,  $\mathbf{S}=0$  and the spin-orbit term falls away.

We treat the volume part of the optical potentials in the initial and the exit channels on the same footing by application of the hybrid nucleus-nucleus optical potential.

The hybrid nucleus-nucleus optical potential [23] has real and imaginary parts:

$$U(\mathbf{r}) = N^R V^{\text{DF}}(\mathbf{r}) + iN^I W(\mathbf{r}). \quad (9)$$

The parameters  $N^R$  and  $N^I$  correct the strength of the microscopically calculated real  $V^{\text{DF}}$  and imaginary  $W$  constituents of the whole potential. They are usually adjusted comparing calculations of elastic cross sections to experimental data in the corresponding channels. The real part  $V^{\text{DF}}$  is a double-folding potential that consists of direct and exchange components:

$$V^{\text{DF}}(\mathbf{r}) = V^D(\mathbf{r}) + V^{\text{EX}}(\mathbf{r}), \quad (10)$$

with

$$V^D(\mathbf{r}) = \int d\mathbf{r}_p d\mathbf{r}_t \rho_p(\mathbf{r}_p) \rho_t(\mathbf{r}_t) v_{NN}^D(\mathbf{s}). \quad (11)$$

The exchange potential is

$$\begin{aligned} V^{\text{EX}}(\mathbf{r}) &= \int d\mathbf{r}_p d\mathbf{r}_t \rho_p(\mathbf{r}_p, \mathbf{r}_p + \mathbf{s}) \rho_t(\mathbf{r}_t, \mathbf{r}_t - \mathbf{s}) \\ &\quad \times v_{NN}^{\text{EX}}(s) \exp \left[ \frac{i\mathbf{K}(\mathbf{r}) \cdot \mathbf{s}}{M} \right], \end{aligned} \quad (12)$$

where  $\mathbf{s} = \mathbf{r} + \mathbf{r}_t - \mathbf{r}_p$  is the vector between the projectile and target nucleons. The reduced mass coefficient is  $M = A_p A_t / (A_p + A_t)$ , where  $A_p$  and  $A_t$  refer to the projectile and target atomic mass numbers. The radial part of the nucleus-nucleus momentum  $K(r)$  is determined as follows:

$$K(r) = \left\{ \frac{2Mm}{\hbar^2} [E - V^{\text{DF}}(r) - V_c(r)] \right\}^{1/2}. \quad (13)$$

where  $V_c$  is the Coulomb potential and  $m$  is the nucleon mass. The quantities  $\rho_p(\mathbf{r}_p)$  and  $\rho_t(\mathbf{r}_t)$  are their density

distributions,  $\rho_p(\mathbf{r}_p, \mathbf{r}_p + \mathbf{s})$  and  $\rho_t(\mathbf{r}_t, \mathbf{r}_t - \mathbf{s})$  are the density matrices, which are approximated as in Ref. [29]. The CDM3Y6-type effective  $N$ - $N$  potentials  $v_{NN}^D$  are based on the Paris  $N$ - $N$  potential determined in Ref. [21].

For the initial channel calculations,  $\rho_t$  for  $^{93}\text{Nb}$  was taken as the standard Fermi form, with parameters from Ref. [30]. In the exit channel a Fermi-form density with parameters from Ref. [31] was adopted for  $^{90}\text{Zr}$ , and the  $^4\text{He}$  density from Ref. [32] was used.

The imaginary part of the optical potential  $W(\mathbf{r})$  in Eq. (9) may have the same form as its real counterpart  $V^{\text{DF}}$ , or can be calculated separately within the high-energy approximation [33] as it was developed in Ref. [23].

The microscopic optical potential obtained in the high-energy approximation in the momentum space has the form:

$$U_{\text{opt}}^H(\mathbf{r}) = -\frac{E}{k} \bar{\sigma}_N (i + \bar{\alpha}_N) \frac{1}{(2\pi)^3} \times \int d\mathbf{q} e^{-i\mathbf{q} \cdot \mathbf{r}} \rho_p(\mathbf{q}) \rho_t(\mathbf{q}) f_N(q). \quad (14)$$

Here the  $N$ - $N$  total scattering cross section  $\bar{\sigma}_N$  and the ratio of real to imaginary parts of the forward  $N$ - $N$  amplitude  $\bar{\alpha}_N$  is averaged over the isospins of the projectile and target nuclei. They are parameterized as given in Refs. [34, 35]. The  $N$ - $N$  form factor is taken as  $f_N(q) = \exp(-q^2 \beta_N/2)$  with the slope parameter  $\beta_N = 0.219 \text{ fm}^2$  [36]. In fact, we used only the imaginary part of Eq. (14).

For the potential in the  $p+^{93}\text{Nb}$  channel, the functions  $\rho_p(\mathbf{r}_p)$  in Eqs. (11) and (12) have to be excluded together with the elementary volumes  $d\mathbf{r}_p$ . Also, in Eq. (14),  $\rho_p(\mathbf{q})$  should not appear.

The shape of the analyzing power is rather sensitive to the spin-orbit part of the optical potential in the initial channel. Good agreement with the experimental data was obtained by using for protons a Woods-Saxon shape of the real part of  $V_{\text{SO}}(r)$ . We used the parameters listed in Ref. [37].

The renormalization constants  $N^R$  and  $N^I$  in the initial channel cannot be defined independently since there are no the respective data on elastic scattering. Therefore they are kept equal to unity, while for the exit channel we need to adjust them to follow the emission-energy trend of the experimental analyzing power data. Very good agreement with the experimental data for the highest emission energy  $E_{\text{out}}=98 \text{ MeV}$  can be obtained if the values of  $N^R$  and  $N^I$  for the exit channel are kept equal to unity as well. For the rest of the outgoing energies we used the values  $N^R=1$  and  $N^I=2$ . Fig. 2 demonstrates the effect which the value of  $N^I$  has on the differential cross section and the analyzing power of the reaction at 86 MeV emission energy. Only the pickup component of the reaction mechanism is used to illustrate the sensitivity to the renormalization of the imaginary potential.

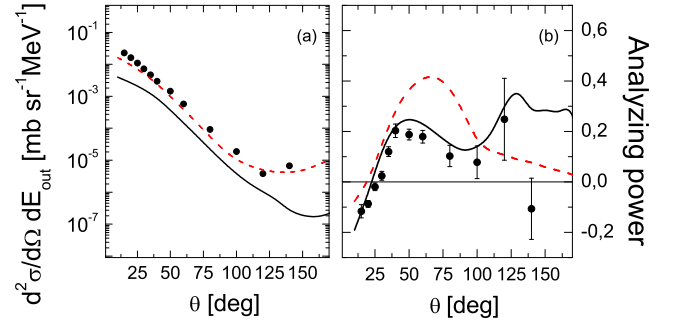


FIG. 2. (Color online) Double-differential cross section (a) and analyzing power (b) as a function of scattering angle  $\theta$  for the  $^{93}\text{Nb}(p,\alpha)$  reaction at an incident energy of 100 MeV and an  $\alpha$ -particle emission energy of 86 MeV. Theoretical cross section and analyzing power calculations for  $N^I=1$  (---) and  $N^I=2$  (solid line) in Eq. (9) are compared with the experimental data. Results for only the pickup component of the reaction mechanism are used to display the trends.

The values found in our present investigation demonstrate that the hybrid optical potential which we use is appropriate for the energy range we consider, although they are not consistent with those for the  $^{93}\text{Nb}(\bar{p},\alpha)$  reaction at incident energy of 160 MeV [15]. Clearly, a further theoretical analysis and complementary experimental studies for proper evaluation and interpretation are needed.

### E. Reaction Mechanism

The mechanism of the direct  $(p,\alpha)$  reaction has been discussed intensively over the years. For example in Refs. [18, 38] the multistep direct reaction theory analysis of  $(\bar{p},\alpha)$  reactions at 65 MeV and 72 MeV incident energies suggested that the reaction mechanism should be a pickup of a triton. In Ref. [39] the authors show that calculations assuming pickup of a triton and knockout of an  $\alpha$  particle equally well fit the angular distribution and the analyzing power of  $^{90,92}\text{Zr}(p,\alpha)$  reaction to the ground state and the first few excited states, while in Ref. [40] the knockout mechanism is preferred for describing transitions to the continuum. In Ref. [15] we considered proton induced  $\alpha$ -particle emission at 160 MeV incident energy and a wide range of emission energies. The existence of experimental data for just forward angles did not allow us to make decisive conclusion about the reaction mechanism, but the calculations assuming that the ejectile originates from an  $\alpha$ -cluster knockout in the final stage reproduce roughly the angular distributions of the measured cross section and analyzing power as a function of  $\alpha$ -particle emission energy.

The history of this debate suggests that it would be wise to consider DWBA calculations for both reaction mechanisms. The theoretical results may then be compared with experimental data of the differential cross sec-

tion and the analyzing power where the first step process is expected to dominate. At an incident energy of 100 MeV this is true at the highest  $\alpha$ -particle emission energy of 98 MeV that is available. Numerically the difference between both types of calculations lies in the form factor, the incoming and the outgoing distorted waves are calculated using the same optical model potentials for protons and  $\alpha$  particles respectively. The proton-triton binding potential has a Woods-Saxon shape with geometrical parameter  $r_0 = 1.87$  fm and  $a = 0.7$  fm, whereas to calculate the  $\alpha$ -particle form factor we use the generally accepted geometrical parameter values of  $r_0 = 1.25$  fm and  $a = 0.65$  fm.

As is seen in Fig. 3, panel (a), the theoretical double-differential cross sections have rather different shapes for a knockout or pickup reaction mechanism. Whereas the pickup cross section can be scaled to fit the forward angles, the knockout cross section reproduces the experimental data very well at larger angles. The sum of the cross sections originating from both reaction mechanisms is required for a good fit to the complete set of experimental data over the whole range of scattering angles. The scaling factors, which are needed to fit the experimental differential cross sections at 98 MeV emission energy, are kept unchanged for the rest of the calculations at other outgoing energies.

Panel (f) of Fig. 3 shows the analyzing power as a function of the scattering angle for pickup (pu) and knockout (ko) reaction mechanisms. The solid line in the figure represents the sum of both distributions, defined as follows:

$$A_{\text{total}} = \frac{A_{\text{pu}} \left( \frac{d^2\sigma}{d\Omega dE} \right)^{\text{pu}} + A_{\text{ko}} \left( \frac{d^2\sigma}{d\Omega dE} \right)^{\text{ko}}}{\left( \frac{d^2\sigma}{d\Omega dE} \right)^{\text{pu}} + \left( \frac{d^2\sigma}{d\Omega dE} \right)^{\text{ko}}}, \quad (15)$$

where the subscripts and superscripts refer to either pickup or knockout, as the abbreviated notations imply.

The analyzing power distribution calculated assuming only pickup reproduces the complete set of experimental data reasonably well, but inclusion of the knockout contribution is crucial. Clearly, both reaction mechanisms play an important role in the theoretical description of the  $^{93}\text{Nb}(p,\alpha)$  pre-equilibrium reaction. Their different contributions under various kinematical conditions are very noticeable.

Many superficially equivalent, yet inherently very different sets of optical potentials which all successfully reproduce elastic scattering are available for generating distorted waves in DWBA calculations of pre-equilibrium reactions. However, as was pointed out in for example Ref. [9], because of known problems, caution is advisable in the choice of a specific set for pre-equilibrium reactions. For application to pre-equilibrium reactions, the optical potentials must be valid over a large range of incident and emission energies. Furthermore, to be generally useful, a wide variety of target nuclei and different ejectiles need to be covered by a single optical potential set. The

possible simultaneous importance of all these characteristics is suggested by the observation (see for example Refs. [10, 14]) that experimental pre-equilibrium cross section distributions of all types appear to follow closely the simple phenomenological systematics of Kalbach [41]. Consequently, implementation of a single truly global optical potential which satisfy all requirements is highly desirable.

In an earlier  $(p,\alpha)$  investigation [14] we used global phenomenological distorting potentials, but these have now been abandoned in favor of a folding procedure. The reason is that the former potentials are extracted independently for the projectile and for the ejectile from elastic scattering, therefore the relationship between the two sets is unknown. In other words, it is simply not clear whether they form a matched pair, as would be desirable. Furthermore, this relationship cannot be readily checked for a reaction into the continuum, as for transfer to a discrete final state. Consequently, in addition to those properties already discussed at the beginning of this subsection, an optimal optical potential should for our present needs offer a good description of elastic scattering for proton projectiles as well as  $\alpha$ -particles (and also for  $^3\text{He}$  to link up to our ongoing two-nucleon transfer studies). A folding procedure comes close to satisfying all the criteria, but unfortunately as we have seen, at the cost of two free parameters, of which one needs to be adjusted in this work. Nevertheless, as was already mentioned earlier, this specific type of folding potential has been successfully employed in the past for pre-equilibrium reactions and, of course, for elastic scattering.

#### F. Influence of momentum mismatch between entrance- and exit channels

Proton-induced multi-nucleon transfer reactions suffer from severe momentum mismatch between the incident- and outgoing channels, which becomes progressively worse with increasing projectile energy. For this reason it is generally accepted that reactions such as  $(p,t)$  and  $(p,\alpha)$  cannot, even at low incident energies, provide reliable spectroscopic information.

At the incident energies investigated in this work the momentum mismatch is in the range of 400 to 600 MeV/c. At those momenta the asymptotic tail of the bound-state wave function has decreased by many orders of magnitude from its maximum. Within normal uncertainties this means that, for all practical purposes, the true value of the bound-state wave function is unknown at the specific momentum range for which the cross section is sensitive. Consequently, under those conditions extremely small errors on the bound state influence cross-section values calculated in DWBA enormously, rendering predicted absolute values meaningless. Fortunately this difficulty does not influence the shape of the angular distribution appreciably (see for example Ref. [42]), therefore analyzing power, which is a ratio of cross sec-



tions, is unaffected by the problem.

To address the problem in this work, we simply normalize our theoretical DWBA cross-section values to the experimental pre-equilibrium angular distributions where the reaction mechanism is likely to be purely of a direct one-step nature in other words at the highest emission energies. The same normalization is used at lower emission energies where multistep contributions, which may be associated with lower initial nucleon driving energies, become relevant. Clearly our procedure only partially solves the problem towards lower emission energies, because it is not known to what extent the adopted bound state reproduces the true trend of the bound-state wave function towards lower incident energy correctly.

A recent investigation [42] of the  $^{58}\text{Ni}(p, ^3\text{He})^{56}\text{Co}$  reaction to discrete final states, which allows an accurate extraction of the trend with incident energy, suggests that our simplistic procedure could easily lead to a cross-section discrepancy as large as observed in the present study at an incident energy of 100 MeV, as will be quantified later. This will be discussed later.

#### IV. RESULTS AND DISCUSSION

We summarize the results of our calculations in Fig. 3 where the double-differential cross section and analyzing power angular distributions for the  $^{93}\text{Nb}(p, \alpha)$  reaction at an incident energy of 100 MeV for various outgoing energies of the  $\alpha$  particles are displayed.

Experimental data are available for outgoing energies starting from 98 MeV (with 106 MeV as a kinematic limit due to a positive  $Q$ -value of the reaction of 6.4 MeV) down to 34 MeV. We have chosen the ones shown in the figure because they are representative of the contribution of both reaction mechanisms to the total differential cross section and analyzing power, respectively. The theoretical results are in good agreement with the experimental quantities, although we have to keep in mind that we have fitted some of the input ingredients of the theory, as implied in Sec. III.

All the theoretical double-differential cross section distributions were normalized with the factors extracted from the angular distributions at an emission energy  $E_{\text{out}}$  of 98 MeV, for which the one-step reaction dominates, as explained in Sec. IIIE. Although the fitting procedure is based on theoretical considerations, it is still somewhat arbitrary. As we explained in Ref. [15], experimental uncertainties in, for example, the emission energy calibration would result in a systematic error in the measured cross section which rapidly gets worse towards the top end of emission energies. The reason is that the energy distribution of the cross section as function of emission energy drops very rapidly to zero as the kinematic limit is approached, whereas it varies considerably more slowly at lower emission energies. Our cross section data, for an incident energy of 100 MeV, at the highest emission energy is already in an energy range where a rapid vari-

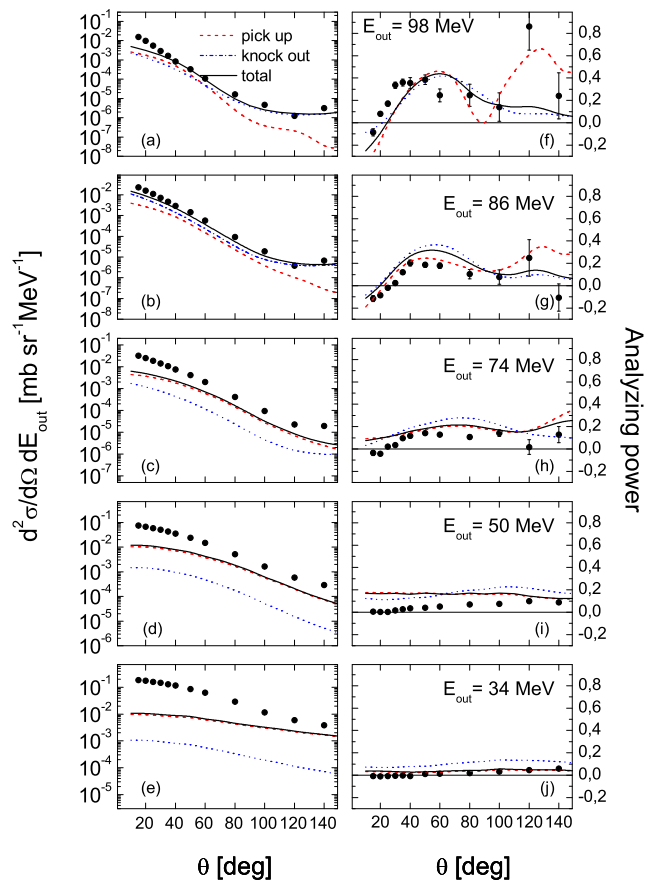


FIG. 3. (Color online) Double-differential cross sections (a)-(e) and analyzing power (f)-(j) as a function of scattering angle  $\theta$  for the  $^{93}\text{Nb}(p, \alpha)$  reaction at an incident energy of 100 MeV and various  $\alpha$ -particle emission energies  $E_{\text{out}}$  as indicated. Theoretical cross section calculations for pickup (---) and knockout (- · -) are shown, with the sums of both reaction mechanisms plotted as continuous curves. The experimental analyzing power distributions are compared with theoretical calculations for pickup (---), knockout (- · -) and the sum of both reaction mechanisms (solid lines).

ation occurs. This, combined with the experimental uncertainty in emission energy, could affect the reliability of the normalization procedure.

A noticeable trend displayed in Fig. 3 is that the theoretical cross sections underestimate the experimental values increasingly towards lower emission energies. As discussed in Sec. IIIF this could perhaps be a normal phenomenon caused by inadequacies in the way that the effect of momentum mismatch is compensated. However, other possible causes should also be considered. It is significant that a similar trend with emission energy was observed even more severely in our other  $(p, \alpha)$  studies at higher incident energy [14, 15]. In one of these investigations [15] the same folding procedure as in this work was used to generate distorting potentials, whereas in the other study [14] normal global phenomenological optical potentials were employed. The similarity of the

discrepancy encountered in the two cases would seem to rule against the specific choice of optical potential in this work as a possible cause of the difficulty. A different issue, unrelated to the optical potential, is that  $\alpha$ -particle evaporation from a compound nucleus could in principle contribute to the continuum yield, thus explaining the observed under-prediction. However, explicit calculation shows that such mechanism contributes only a fraction of a percent [43] to the total angle-integrated cross section at the lowest emission energy of Fig. 3. An isotropic distribution for the evaporation component still implies that it contributes less than 1% to the yield even at the most backward angle. A similar negligible contribution is present at an incident energy of 65 MeV and at an emission energy of 37 MeV, which will be explored later. In other words,  $\alpha$ -particle evaporation from compound-nuclear decay definitely does not distort any of the angular distributions displayed in this work.

As was mentioned earlier, and also as was pointed out in Ref. [15], because the analyzing power consists essentially of a ratio of cross sections, it would not be appreciably affected by most of the putative causes of a cross section problem. It is significant that the experimental analyzing-power angular distributions are reproduced well by the theory over the whole range of emission energies explored. Because we overwhelmingly base our conclusions regarding the reaction mechanism on features observed in analyzing power distributions, we do not consider the cross section under-prediction to be a serious concern.

As is also shown in Fig. 3, the differential cross sections of the knockout reaction mechanism decrease faster than those for pickup towards lower emission energies. Therefore, on average the total differential cross section is dominated by the pickup contribution at an incident energy of 100 MeV.

To extend the study of the  $^{93}\text{Nb}(p,\alpha)$  reaction to a lower incident energy we re-examined the experimental data by Sakai *et al.* [16], where the differential cross section and the analyzing power distributions of the continuum spectra for various target nuclei including  $^{93}\text{Nb}$  were measured for 65 MeV polarized protons in a wide range of excitation energies and angles.

Our further investigation of the  $^{93}\text{Nb}(p,\alpha)$  reaction at 65 MeV incident proton energy and at three outgoing energies followed the same procedures as those described in Sec. III. It turned out that for this incident energy the knockout mechanism is sufficient to describe the available experimental data. Not only does a pickup mechanism give inferior agreement with the experimental angular distributions, but any combination of pickup and knockout fails to achieve better results than knockout by itself.

The comparison of the experimental and theoretical double-differential cross section and analyzing power is shown in Fig. 4. First of all we should point out that the theoretical calculations reproduce the shape of the differential cross section at the largest outgoing energy

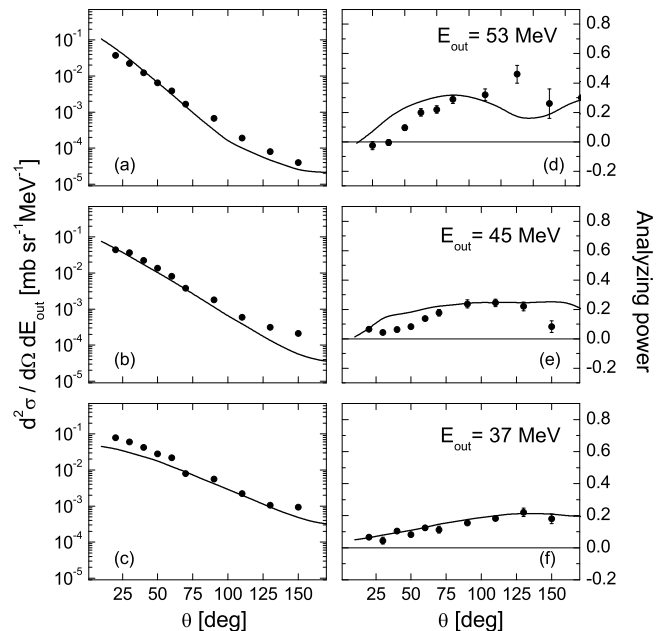


FIG. 4. Double-differential cross sections (a)-(c) and analyzing power (d)-(f) as a function of scattering angle  $\theta$  for the  $^{93}\text{Nb}(p,\alpha)$  reaction at an incident energy of 65 MeV and various  $\alpha$ -particle emission energies  $E_{\text{out}}$  as indicated. Theoretical calculations for a knockout reaction mechanism (solid line) are compared with the experimental data by Sakai *et al.* [16].

of 53 MeV very well. Once fitted at this emission energy the magnitudes of the differential cross section are in very good agreement with the experimental data at lower emission energies as well. We may speculate that this is because we treat all important intranuclear processes properly, but we should also keep in mind that we determine the scaling factor at an emission energy as much as 18 MeV lower than the kinematic limit, where the first-step direct knockout is no longer the only kinematically allowed process. Furthermore, we also explore a very limited emission-energy range of only 16 MeV, as provided by the available experimental data. Nevertheless, the magnitude and shape of the cross section, as well as the shape of the analyzing power distributions are reproduced remarkably well at all emission energies which are available. Consequently we can confidently claim that at 65 MeV incident energy the  $^{93}\text{Nb}(p,\alpha)$  reaction is described mainly by a knockout reaction mechanism.

These data of Sakai *et al.* [16] at an incident energy of 65 MeV have also been investigated by Tamura *et al.* [38]. It is beyond the scope of the present work to discuss details of the calculations of Ref. [38] in such a way that a proper comparison with our results is meaningful. Nevertheless, it is noteworthy that the analyzing power angular distributions are reproduced considerably better in our work.

An interesting feature of the theoretical cross section angular distributions in Fig. 3, for an incident energy



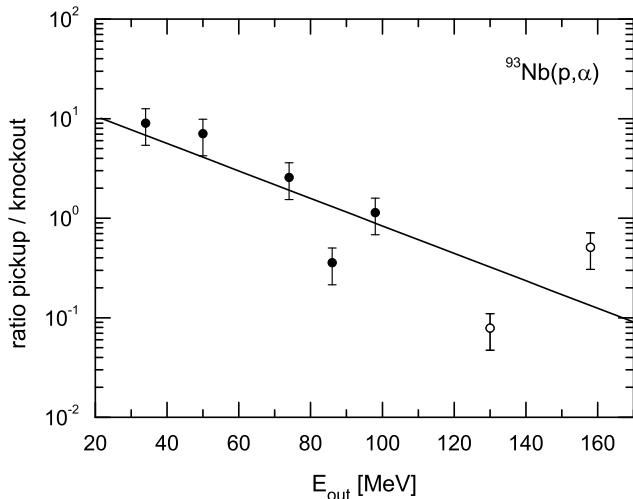


FIG. 5. Ratio of cross sections for pickup and knockout as a function of  $\alpha$ -particle emission energy  $E_{out}$ . Solid circles represent results for an incident energy of 100 MeV, and open circles are for 160 MeV from previous work [15]. Error bars are only rough estimates, and the curve is an exponential fit to the data.

of 100 MeV, is that the magnitudes for knockout drop off more rapidly with decreasing emission energy than those of pickup. This is plotted in Fig. 5 as the ratio of pickup to knockout as a function of emission energy. Of course the shapes of the two distributions differ somewhat, therefore the most forward angle at which experimental data were measured was arbitrarily chosen for the comparison. Clearly the observed trend would be only slightly influenced by this specific choice. We find that for an incident energy of 100 MeV pickup becomes more important with decreasing emission energy. Of course, emission energy is simply related to incident energy, but due to the changing contributions from different reaction steps, one should not simply infer from this that pickup should be even more important at 65 MeV than at 100 MeV incident energy. In fact, we find the opposite. As shown in Fig. 5, the result from our previous study [15] at 160 MeV does indeed seem to support such a naive incident-energy dependence. However this result may be spurious if we consider the large systematic uncertainty in the extracted ratio in that case. At 100 MeV incident energy, not only is the systematic uncertainty much smaller, but the trend is very reliable.

Our current optical potentials do not comprise a surface imaginary component. This neglect could in principle become an increasing problem towards lower incident energies. Evidence of the importance of such deficiency would presumably have revealed itself at 65 MeV as a worsening agreement between the theoretical and experimental distributions, or perhaps as an unfavorable comparison of our results with those of Tamura *et al.* [38], in whose work surface effects are included. We reassuringly find exactly the opposite in both cases. We should men-

tion that, as a whole, our various pre-equilibrium studies published elsewhere [8–11, 14, 15] do not seem to show a qualitative sensitivity to the exact choice of any reasonable optical potential. This may be because the multi-step character of the reaction mechanism puts a powerful stamp on the features of the experimental observables.

## V. SUMMARY AND CONCLUSIONS

Cross section and analyzing-power angular distributions for the reaction  $^{93}\text{Nb}(\vec{p}, \alpha)$  at a projectile energy of 100 MeV and various  $\alpha$ -particle emission energies from 98 MeV down to 34 MeV were presented. The experimental angular distributions were compared with the predictions of a statistical multistep direct emission. Reasonable agreement was found between theoretical and experimental results if both knockout as well as pickup are included as mechanisms leading to the final emission of  $\alpha$  particles.

The same theoretical analysis was extended to existing experimental results [16] for the same reaction at a lower projectile energy at 65 MeV. The predicted cross section and analyzing-power angular distributions were again in very good agreement with the experimental data. However, at this incident energy, a strong preference was found for a knockout process. This finding is in agreement with our earlier work at an incident energy of 160 MeV [15].

Evidently the reaction mechanism in the  $^{93}\text{Nb}(\vec{p}, \alpha)$  reaction changes from a dominant knockout process at 65 MeV incident energy, to a combination of pickup and knockout participating at 100 MeV, and then back to only knockout being important at 160 MeV. The usual assumption is that a target such as  $^{93}\text{Nb}$  is representative of nuclei in general as far as the pre-equilibrium  $(p, \alpha)$  reaction is concerned. However, the present conclusion regarding the change in the ratio of participating mechanisms for this target needs to be confirmed for other nuclear species.

As in other investigations of the  $(p, \alpha)$  reaction [14, 15], at 100-MeV incident energy it is found that the absolute cross section is increasingly under-predicted towards lower emission energies. Although comparisons between experimental and theoretical analyzing power results suggest that this is not a serious concern, it would be advisable to investigate the lower-than-expected theoretical cross sections further. Based on the trend from comparable  $(p, ^3\text{He})$  [8–11] and  $(p, \alpha)$  [14, 15] studies in the 100 MeV to 200 MeV incident-energy range, it is reasonable to speculate that the issue which is encountered in the magnitude of the predicted cross section is mainly related to problems with proton-induced multi-nucleon transfer reactions in general. For example, it is well known that severe momentum mismatch in  $(p, \alpha)$  reactions to discrete final states makes it difficult, if not impossible, to extract spectroscopic information. This is caused by sensitivity of the cross section to the asymptotic region of the bound

state wave function, due to momentum mismatch, which is sampled by a  $(p, \alpha)$  reaction.

Clearly, it would be informative to explore the issues found in the present investigation for other targets. Experimental as well as further theoretical work should be invaluable.

## ACKNOWLEDGMENTS

Our appreciation is extended to G. F. Steyn and S. V. Förtsch for providing the numerical data at an incident

energy of 100 MeV reported in this work. The research of A.A.C. was funded by the National Research Foundation (NRF) of South Africa. The studies of S.S.D. were partially supported by the SARFEN grant of the Bulgarian Science Foundation. E.V.Z. and K.V.L. were supported by the Russian Foundation for Basic Research (RFBR) under Grants No. 12-01-00396a and No. 13-01-00060a. This financial support is gratefully acknowledged.

- 
- [1] E. Gadioli and P. E. Hodgson, *Pre-Equilibrium Nuclear Reactions* (Oxford University Press, New York, 1991).
  - [2] A. J. Koning and J. M. Akkermans, *Phys. Rev. C* **47**, 724 (1993).
  - [3] H. Feshbach, A. Kerman and S. Koonin, *Ann. Phys. (N. Y.)* **125**, 429 (1980).
  - [4] W. A. Richter, S. W. Steyn, A. A. Cowley, J. A. Stander, J. W. Koen, R. Lindsay, G. C. Hillhouse, R. E. Julies, J. J. Lawrie, J. V. Pilcher, and P. E. Hodgson, *Phys. Rev. C* **54**, 1756 (1996).
  - [5] W. A. Richter, A. A. Cowley, G. C. Hillhouse, J. A. Stander, J. W. Koen, S. W. Steyn, R. Lindsay, R. E. Julies, J. J. Lawrie, J. V. Pilcher, and P. E. Hodgson, *Phys. Rev. C* **49**, 1001 (1994).
  - [6] W. A. Richter, A. A. Cowley, R. Lindsay, J. J. Lawrie, S. V. Förtsch, J. V. Pilcher, R. Bonetti, and P. E. Hodgson, *Phys. Rev. C* **46**, 1030 (1992).
  - [7] A. A. Cowley, A. van Kent, J. J. Lawrie, S. V. Förtsch, D. M. Whittall, J. V. Pilcher, F. D. Smit, W. A. Richter, R. Lindsay, I. J. van Heerden, R. Bonetti, and P. E. Hodgson, *Phys. Rev. C* **43**, 678 (1991).
  - [8] A. A. Cowley, G. J. Arendse, G. F. Steyn, J. A. Stander, W. A. Richter, S. S. Dimitrova, P. Demetriou, and P. E. Hodgson, *Phys. Rev. C* **55**, 1843 (1997).
  - [9] A. A. Cowley, G. F. Steyn, S. S. Dimitrova, P. E. Hodgson, G. J. Arendse, S. V. Förtsch, G. C. Hillhouse, J. J. Lawrie, R. Neveling, W. A. Richter, J. A. Stander, and S. M. Wyngaardt, *Phys. Rev. C* **62**, 064605 (2000).
  - [10] A. A. Cowley, J. Bezuidenhout, S. S. Dimitrova, P. E. Hodgson, S. V. Förtsch, G. C. Hillhouse, N. M. Jacobs, R. Neveling, F. D. Smit, J. A. Stander, G. F. Steyn, and J. J. van Zyl, *Phys. Rev. C* **75**, 054617 (2007).
  - [11] A. A. Cowley, J. J. van Zyl, S. S. Dimitrova, E. V. Zemlyanaya and K. V. Lukyanov, *Phys. Rev. C* **85**, 054622 (2012).
  - [12] E. Renshaw, S. J. Yennello, K. Kwiatkowski, R. Planeta, L. W. Woo, and V. E. Viola, *Phys. Rev. C* **44**, 2618 (1991).
  - [13] A. A. Cowley and J. J. van Zyl, *EPJ Web of Conferences*, **66**, 03020 (2014).
  - [14] A. A. Cowley, G. J. Arendse, J. W. Koen, W. A. Richter, J. A. Stander, G. F. Steyn, P. Demetriou, P. E. Hodgson, and Y. Watanabe, *Phys. Rev.* **54**, 778 (1996).
  - [15] S. S. Dimitrova, A. A. Cowley, J. J. van Zyl, E. V. Zemlyanaya, and K. V. Lukyanov, *Phys. Rev. C* **89**, 034616 (2014).
  - [16] H. Sakai, K. Hosono, N. Matsuoka, S. Nagamachi, K. Okada and K. Maeda, H. Shimizu, *Nucl. Phys. A* **344**, 41 (1980).
  - [17] J. V. Pilcher, A. A. Cowley, D. M. Whittall, and J. J. Lawrie, *Phys. Rev. C* **40**, 1937 (1989).
  - [18] Z. Lewandowski, E. Loeffler, R. Wagner, H. H. Mueller, W. Reichart and P. Schober, *Nucl. Phys. A* **389**, 247 (1982).
  - [19] P. D. Kunz and E. Rost, in *Computational Nuclear Physics*, edited by K. Langanke *et al.* (Springer-Verlag, Berlin, 1993) Vol. 2, Chap. 5.
  - [20] R. Bonetti, L. Colli Milazzo, I. Doda, and P. E. Hodgson, *Phys. Rev. C* **26**, 2417 (1982).
  - [21] D. T. Khoa and G. R. Satchler, *Nucl. Phys. A* **668**, 3 (2000).
  - [22] P. Shukla, *Phys. Rev. C* **67**, 054607 (2003).
  - [23] V.K. Lukyanov, E. V. Zemlyanaya, and K.V. Lukyanov, *JINR Preprint P4-2004-115* (Joint Institute for Nuclear research, Dubna, 2004); *Phys. At. Nucl.* **69**, 240 (2006).
  - [24] K. V. Lukyanov, *Comm. JINR, P11-2007-38* (Joint Institute for Nuclear Research, Dubna, 2007).
  - [25] K. V. Lukyanov, V. K. Lukyanov, E. V. Zemlyanaya, A. N. Antonov, and M. K. Gaidarov, *Eur. Phys. J.* **A33**, 389 (2007).
  - [26] V. K. Lukyanov, E. V. Zemlyanaya, K. V. Lukyanov, D. N. Kadrev, A. N. Antonov, M. K. Gaidarov, and S. E. Massen, *Phys. Rev. C* **80**, 024609 (2009).
  - [27] V. K. Lukyanov, D. N. Kadrev, E. V. Zemlyanaya, A. N. Antonov, K. V. Lukyanov, and M. K. Gaidarov, *Phys. Rev. C* **82**, 024604 (2010).
  - [28] V. K. Lukyanov, D. N. Kadrev, E. V. Zemlyanaya, A. N. Antonov, K. V. Lukyanov, M. K. Gaidarov, and K. Spasova, *Phys. Rev. C* **88**, 034612 (2013).
  - [29] J. W. Negele and D. Vautherin, *Phys. Rev. C* **5**, 1472 (1972).
  - [30] J. D. Patterson and R. J. Peterson, *Nucl. Phys. A* **717**, 235 (2003).
  - [31] M. El-Azab and G. R. Satchler, *Nucl. Phys. A* **438**, 525 (1985).
  - [32] V. V. Burov, V. K. Lukyanov, *JINR Preprint P4-11098* (Joint Institute for Nuclear Research, Dubna, 1977).
  - [33] R. J. Glauber, *Lectures in Theoretical Physics* (New York, Interscience, 1959), p. 315.
  - [34] S. K. Charagi and S. K. Gupta, *Phys. Rev. C* **41**, 1610 (1990); **46**, 1982 (1992).
  - [35] P. Shukla, arXiv:nucl-th/0112039.

- [36] G. D. Alkhazov, S. L. Belostotsky, and A. A. Vorobyov, Phys. Rep. **42**, 89 (1978).
- [37] F. D. Becchetti Jr. and G. W. Greenlees, Phys. Rev. **182**, 1190 (1969).
- [38] T. Tamura, H. Lenske and T. Udagawa, Phys. Rev. C **23**, 2769 (1981).
- [39] E. Gadioli, E. Gadioli-Erba, P. Guazzoni, P. E. Hodgson, and L. Zetta, Z. Phys. A **318**, 147 (1984).
- [40] R. Bonetti, F. Crespi, and K.-I. Kubo, Nucl. Phys. A **499**, 381 (1989).
- [41] C. Kalbach, Phys. Rev. C **37**, 2350 (1988).
- [42] J. J. van Zyl, Ph.D. thesis, Stellenbosch University (2012).
- [43] A. J. Koning and D. Rochman, Nuclear Data Sheets **113**, 2841 (2012); A. J. Koning, D. Rochman, S. van der Marck, J. Kopecky, J. Ch. Sublet, S. Pomp, H. Sjostrand, R. Forrest, E. Bauge and H. Henriksson, [www.talys.eu/tendl-2012.html](http://www.talys.eu/tendl-2012.html).